ALUMINUM AND IRON OXI-HYDROXIDE SEGREGATION IN NODULES OF LATOSOLS DEVELOPED ON TERTIARY SEDIMENTS (BARREIRAS GROUP), NEAR MANAUS (AMAZON BASIN), BRAZIL*

A. CHAUVEL[1], R. BOULET[2], P. JOIN[3] AND G. BOCQUIER[3]

1 - ORSTOM/IG-USP - São Paulo, Brazil
2 - ORSTOM Cayenne, Guyane Française
3 - Université de Paris VII, France

ABSTRACT

The clayey latosols from the northern part of Manaus, are developed in low table-lands made of detritic continental sediments ("Barreiras" tertiary).

With a depth of 3 to 4 meters, these soils have in fact as parental material the products coming from mineralogical transformations of these sediments (intense dissolution of the quartz, aluminium hydroxides concentration, neoformation of kaolinite, ...).

The effect of these transformations increases from bottom to top, starting from a depth of 15 meters up to extremelly clayey material of the soils (70 to 90% of clay).

This pedologic mantle perfectly shapes the surface of the strong sloping convex sides on the limits of the table-lands. At the bottom of this mantle one can observe two distinct sequences of nodular differentition: the first one essentially ferruginous and the second one gibbsitic.

The ferruginous nodules, reddish violet in colour, appear at a depth of aproximately 10 meters under the shape of diffuse volumes; they progressively individualize themselves up to a depth of 3 to 4 meters from the surface, taking vertically elongated forms with concave edges, then they suddenly disappear at aproximately 1.5 meters. The microscopic analysis and microanalysis disclose: 1. that they are in continuity with the surrounding matrix; 2. that they are made of two different types of plasma, the first one isotic and ferruginous (55% of Al_2O_3), the second one crystic and gibbsitic (50% of Al_2O_3); 3. that the transition which divides these two types of plasma within the same nodule is progressive (a sign of a genetic relation between them).

The white gibbsitic nodules progressively individualize themselves from a depth of 4 to 5 meters. At approximately 2 meters they progressively become pale yellow argillous blocks, which constitutes their broken down form. The microscopic analysis and microsonde shows: 1. that these nodules are also themselves, at the same time in morphologic and geochemical continuity with the matrix; 2. that they are made of two types of plasma, one isotrope homogeneous, the other one crystic; 3. that these two plasmas have approximately the same proportions of kaolinite and gibbsite (more or less

* This research has been carried out in the I.N.P.A. (Instituto Nacional de Pesquisas da Amazonia) and has been financially supported by the CNPq-CNRS/ORSTOM Conv.

50% each); 4. that the transition from the first plasma to the second one is only affected by a progressive decrease of the Fe_2O_3 content (from 2 to 0.5%) in line with an increase of the size of the gibbsite crystals, these last ones reaching dimensions and shapes recognizable with an optical microscope only around voids (crystallarias).

A detailed study of these two sequences shows therefore that these ferruginous and gibbsitic nodules, individualize themselves by the effect of mineralogical and structural transformations which, from the "Barreiras" sediment give birth to the parental material of the soil. Afterwards they degrade within the pedological bodies.

Consequently these nodules appear and disappear "in situ", progressively with the lowering of the weathering and pedogenesis profiles in the tertiary continental sediments.

INTRODUCTION

The results presented here concern some pedological profiles located about 100 km north of Manaus (Fig. 1).

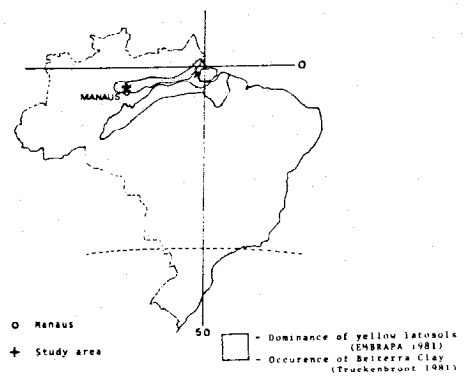

FIG. 1. Locality Map.

The climate is equatorial (Amazonian type with an annual rainfall of 2100 mm and a markedly dry season). The vegetation consists of dense humid evergreen forest. Circulating waters (ground water and rivers) are very pure with a dissolved silica content oscillating between 0.5 and 4.5 ppm (Sioli, 1968).

The latosols of this region (ferrallitic soils according to the French classification and oxisols according to the American classification), described and studied by Sombroek (1966), are developed on a low plateau made up of detrital continental sediment (Tertiary, Barreiras group, Bigarella, 1975).

These profiles consist, from base to top, of 3 main layers: (i) below 9 meters, the parent rock made up of sandy and clayey sediment with a cross-bedded structure; (ii) a ferruginous and aluminous nodular layer about 5 m thick; (iii) a very heavy textured yellow layer (photos 1 and 2).

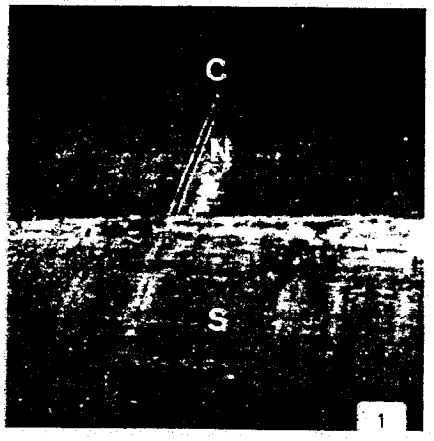

Photo 1. Road Cut. C. Clayey yellow layer; N. Nodular layer: S. Parent sediment

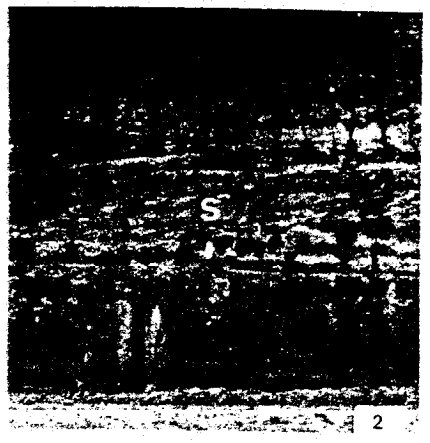

Photo 2. Sediment (S), with a cross bedded structure.

The nodules from layer (ii) were analysed in detail, at their natural environment, mainly by means of microscopical and ultramicroscopical techniques, in order to characterize the relations between these nodules and their "S-matrix".

CHARACTERIZATION OF THE THREE PRINCIPAL LAYERS

The parent sediment and the early stages of transformation

The parent rock mainly consists of heterometrical quartz grains associated with opaque grains of magnetite and a few zircon grains (zircon/quartz ratio of nearly 0.01). These skeletal grains are irregularly scattered among a kaolinite and iron or aluminium oxihydroxide plasma distributed in cutanic pattern. The porosity consists essentially of intergranular and sub-parallel planar voids (in the sense of Brewer, 1964).

One can observe some mineral and structural transformations affecting this sediment. From the base to the top of this layer, they are as follows:

. Plasma ferruginization: the iron oxi-hydroxides which consist of horizontal purplish red bands below the top of fluctuating water table (beneath 14 m) are redistributed first into diffuse brown red spots, then they locate around skeleton grains and voids (photo 5).

. Quartz dissolution: it becomes noticeable with the fragmentation of gravels into

residual undisplaced grains of sand size (photo 3) and with the formation of peripheral voids between quartz and ferruginized plasma (photo 5), thus indicating that the quartz dissolves after ferruginization begins. SEM observations show the etched surface of quartz affected by dissolution (photos 4 and 6).

. Kaolinite neoformation: macroscopically the kaolinite neoformations are revealed by the occurrence of horizontally oriented white lenses of varied dimensions (millimetrical to metrical). Such clayey lenses are almost quartzless and consist of kaolinite. In the microscope (photo 7) or SEM (photo 8), one observes the distribution of this kaolinite and booklets, which may reach 500 µm in maximum dimension (photo 15). This indicates automorphic growth of kaolinite. Moreover, such kaolinite can occur in planar voids (in this case, one observes at the base of the kaolinite lenses a thin skin of argillans also made up of kaolinite) and can penetrate the corrosion vughs affecting the quartz grains. This demonstrates the neoformation of kaolinite as being posterior to the beginning of the quartz dissolution.

Thus, from the cross bedded parent sediment, progressive and continuous transformations appear and develop upward the profile. Such transformations affect both the fabric and the mineral composition of the parent material. They result in a redistribution of iron oxides, a decrease of quartz content, an increase of kaolinite by neoformation and the filling of volumes (intergranular and planar voids).

The nodular layer

The nodules described here are morphologically similar to "hematitic and gibbsitic fragments and granules" observed by Truckenbrodt and Kotschoubey (1981) inside the "Belterra clay" mantle of the bauxitic plateaus of the lower Amazon.

In this nodular layer, one can define several evolutionary stages as follows:

In the lower part of the layer, from 9 to 4 meters deep, the nodules present more or less diffuse outer limits and are little indurated (soft nodules). The porosity is vertical and develop progressively upward along the profile.

In the microscope one clearly observes 3 main transformations which developed from the base to the top of the layer:

. The matrix of sedimentary origin, principally made up of quartz, kaolinite and iron oxi-hydroxides, is affected by progressive increase of ferruginization (photos 9, 10 and 11). Iron concentrations of hematite occur, not only around the quartz grains and the voids (neocutans) but also as irregular scattered spots. All the quartz grains are separated from the plasma by voids. This shows the continuation of quartz dissolution.

. The secondary accumulation of kaolinite (neoformed and cutanic) almost quartzless (photos 15 and 16) are modified by the progressive development of cryptocrystalline patches made up of a mixture of kaolinite, goethite and gibbsite (photo 17). By means of SEM, one can observe (photo 18) that these patches consist in fact of small kaolinite aggregates covered by very fine goethite crystals, and by perfectly clear gibbsite crystals. Towards the top, one observes the continuous transition from this patchy cryptocrystalline material to microcrystalline gibbsitic nodules (photo 19).

. Around the vertical and oblique voids (fissures and channels), the main components of the matrix (quartz, oxi-hydroxides and kaolinite) are mixed in microaggregates (photo 27). This can be attributed to disturbance process (pedoturbation in the sense of Hole, 1961). The detail of such microaggregates can be observed under SEM (photo 28).

In the upper part of the nodular layer, between a depth of 4 m and 2.5 m, as the nodules become more indurated (hard nodules), their boundaries with the environmental S-matrix become clearer. Such an evolution results from mineralogical and structural transformations:

. In the ferruginized matrix of sedimentary origin (photos 12 and 13), one can see first the growth of iron neocutans around the quartz grains. Thus these corroded quartz grains seem to "float" in their ferruginous envelope and are, by this process, isolated from the environmental plasma. In the same way, one observes, not only the development of gibbsite in a crystic fabric in the intergranular volumes, but also large gibbsite crystals lining the voids (photo 14).

. Inside the already partially gibbsitized material (inherited from the secondary accumulations of kaolinite) one observes a generalization of the crystic plasmic fabric at the expense of kaolinite. Moreover crystal size increases, particularly in crystals situated around the voids, until to form crystallarias.

. In the pedoturbed volumes developed along the vertical voids, one observes the formation of strongly lobate voids in pedotubules of biological origin, as shown in other examples by Brewer (1964). These pedotubules locally delineate the outer limits of ferruginous and gibbsitic nodules (photos 29 and 30). One also notes the homogenization of a brownish yellow S-matrix made up of a largely dominant kaolinitic plasma, in which small grains of quartz and fragments of ferric and gibbsitic nodules are scattered.

All the transformations above described lead to the individualization of ferric, gibbsitic and mixed nodules, among a pedoturbed S-matrix.

The chemical composition of these different nodules was studied by means of microprobe (Join, 1980).

a. Inside a mixed nodule (Fig. 2a) - whose plasma is deep red, isotic in the core and whitish, crystic at the periphery - surrounded by a brownish yellow S-matrix, the micro-analyses clearly show that:

. the iron content is greater in the deep red plasma (73% of Fe_2O_3) and progressively decreases toward the whitish crystic plasma (25 to 13%);

. in the whitish crystic plasma, the aluminum content is greater in the central part (50% of Al_2O_3), decreasing progressively on both sides away from this central band

(in all cases such variations are independent of silica variations);

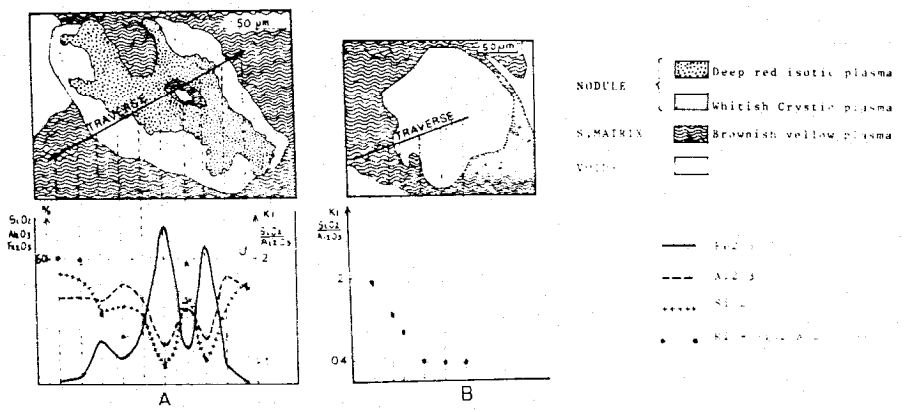

FIG. 2. Electron probe analysis of a mixed ferri-gibbsitic nodule (A) and of a gibbsitic nodule (B) in the S-Matrix.

. the SiO_2/Al_2O_3 ratio progressively increases at the periphery of the nodule, reaching 2 in the surrounding pedoturbed S-matrix (this indicating the predominantly kaolinitic composition of the brownish yellow plasma).

b. A similar progressive increase in SiO_2/Al_2O_3 is observed (Fig. 2b) from the center of a whitish crystic gibbsitic nodule outward into the encasing S-matrix, where the ration reaches a value of 2 (kaolinite). Thus, in this part of the nodular sequence, there is a geochemical continuity, on the one hand, between ferruginous and aluminous concentrations (when they occur together in the same nodule) and on the other, between gibbsitic nodular concentrations and kaolinitic S-matrix.

At the top of the nodular layer, 2.5 m depth, almost all the limits which separate the more indurated concentrations (hematitic-gibbsitic) from the pedoturbed clayey S-matrix are outlined by peripheral fissures (photos 21 and 22) or by pedotubules of biological origin (photo 30). Once formed these discontinuities become increasingly clearer due to smoothing of the surfaces of the fissures and the formation of a superficial ferruginous cortex with a bright, smooth, roundish surface within the indurated concentration. This evolution characterizes the upper part of the nodular layer, in which the content of indurated material reaches its maximum (up to 40% of the weight of the material).

Moreover one also observes the products of degradation of the nodular material in the brownish yellow S-matrix: small fragments of ferruginous concentrations, corroded quartz and microcrystals of gibbsite are scattered around the nodules (photo 23 and 24);

elsewhere one notes the presence of light-coloured crystic and gibbsitic material, with continuous structure, around which radial fissures develop in the S-matrix due to swelling and shrinkage of clayey material (photos 25 and 26).

Thus the microscopic analysis of the top of the nodular layer shows that, for this part of the profile, there occur:

. a relative residual accumulation of the most resistant nodules (predominantly ferruginous);

. a structural and mineralogical degradation of the greater part (predominantly gibbsitic) of the nodular material leading to a mixture of gibbsite, residual quartz and fragments of ferruginous concentrations. This process eventually generates the clayey S-matrix of the upper B2 horizon which is principally made up of kaolinite and small amount of iron and aluminum hydroxides.

The clayey, brown yellow, B2 horizon

In the B2 horizon located immediatly above the nodular level, the largely dominant plasma presents light coloured material with very fine, dispersed gibbsite crystals and plasma separations, and browner bioturbed volumes. It countains some strongly corroded quartz grains (photo 32) with typical dissolution patterns (compare to photo 12) and small hematitic and gibbsitic nodules fragments.

A little higher in the profile, the S-matrix is essentially made up of (i) kaolinitic brownish yellow plasma; (ii) some hematitic and gibbsitic micronodules (more abundant in the pedotubules); (iii) small quartz and zircon grains (photo 31). The zircon/quartz ratio, of nearly 0.03 is three times higher than the one obtained at the lower part of the profile.

DISCUSSION

Figure 3 summarizes the main data obtained in this study. We have tried to present the separate and associated mineralogical and structural transformations that we have recognized from the base to the top of the weathering profile:

. In the lower part of the profile, the parent sedimentary rock presents a porosity consisting almost only of bedding planes. This material, affected by a fluctuating water table, presents:
  . an iron redistribution controled by Eh variations;
  . a progressive dissolution of quartz, which leads to an increase of porosity;
  . an abundant neoformation of automorphic kaolinite which either consists essencially of crystallization from solutions in voids of different origins, or results from a pseudomorphic alteration of the parent materials.

. Above the fluctuating water table, the base of the nodular layer is characterized by the progressive upward development of vertical and oblique porosity, permitting drainage:
  . the iron concentration occurs around skeleton grains and voids of the matrix of

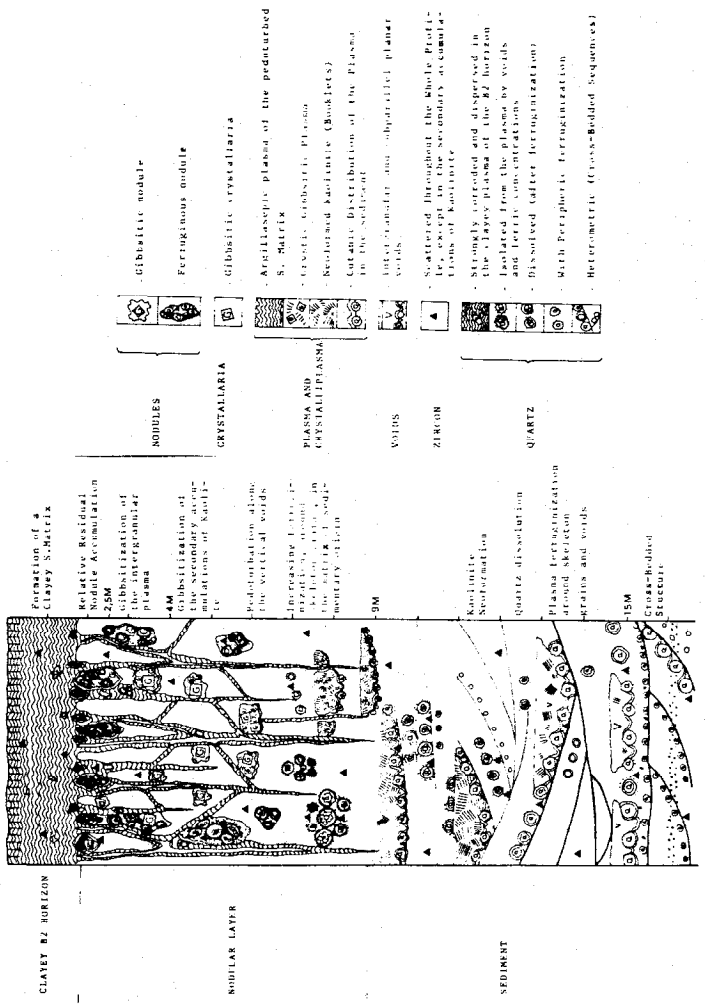

FIG. 3. Schematic representation of the principal structural and mineralogical transformations discussed in this paper.

sedimentary origin;

- the very strong quartz dissolution leads to residual grains that "float" within their ferruginous plasma moulds;
- gibbsite forms initially from the desilification of neoformed kaolinite; eventually, the desilicification process reaches the kaolinite occuring within the S-matrix of sedimentary origin. This difference in order of dissolution of kaolinite may be linked to the absence of quartz in the neoformed volumes; quartz in the S-matrix may protect by its own dissolution, for a time, the kaolinite of sedimentary origin.

The ferruginization and gibbsitization in situ thus lead to the formation of nodules, either ferruginous (issued from the matrix of sedimentary origin), or essentially gibbsitic and quartzless (issued from secondary accumulation of kaolinite), or mixed, including quartz relicts (resulting from the evolution of ferruginous nodules).

From this stage onward, a pedoturbed and porous S-matrix made up of kaolinite and small quartz grains begins to develop around channels and planes.

- In the upper part of the nodular layer a continuous transition occurs between the soft nodules with diffuse limits and the hard nodules with a clear delineation with regard to the S-matrix.
- The nodules which were differentiated from the S-matrix at the base of the layer, are destroyed at the top by physico-chemical processes and supply kaolinite, iron and aluminum oxi-hydroxides and fragments of residual quartz to the S-matrix of the B2 horizon.
- The most resistant, partially destroyed nodules, become concentrated by relative accumulation to form an irregular pebbly layer. Thus the indurated nodules occuring at the top of nodular layers, do not result from an allochthonous origin as could be supposed, but rather result from in situ geochemical evolution.

The percentage of unweathered zircon versus that of dissolved quartz in the pedological profile compared to the ratio in the parent material allows us to conclude that 2/3 of the quartz is eliminated by the weathering process.

Moreover, the appearence and development of gibbsite can be regarded as a relative accumulation of aluminum, principally coming from the desilicification of phyllosilicates. It is only in the upper part of the pedological profile that the gibbsite nodules, in turn, are destroyed. Alumina released this way could be added by absolute accumulation to the underlying layer. We can also suppose that part of this alumina could be transported lower in the profile, or to topographically lower areas, where, in the presence of silica, it could contribute to kaolinite neoformation.

A similar analysis by Muller et al. (1980-1981) on ferrallitic soil developed on Congo granito-gneiss, led to similar conclusions. One may draw analogies between the processes of nodular differentiation that affected, both the crystalline rock of the Congo and the tertiary sediment of the Amazon basin.

LEGEND TO PLATES

For each plate the order of presentation of the figures, from bottom to top, corresponds, to the sequence of mineralogical and structural transformations in the road cut.

PLATE I - THE SEDIMENT (BARREIRAS) AND ITS INITIAL TRANSFORMATIONS (from 15 to 9 meters depth).

Photo 3. Thin section micrograph (plain light): heterometrical quartz (Q), opaque minerals (O) and small zircon grains (Z), cutanic distribution of the plasma (C), intergranular and subparallel voids (V).

Photo 4. Scanning electron micrograph: corroded quartz (Q) enveloped in ferri-argillans (F).

Photo 5. Thin section micrograph (plain light): ferruginous brownish red neocutans (F) around skeleton grains and voids.

Photo 6. SEM: detail of dissolved quartz grain (Photo 4). Etching pattern in which the crystalline form of quartz tends to be developed and emphasized; ferriargillan (F).

Photo 7. Thin section micrograph (crossed nicols): booklets of kaolinite (K) in almost quartzless material.

Photo 8. SEM: automorphic booklets of kaolinite.

PLATE I

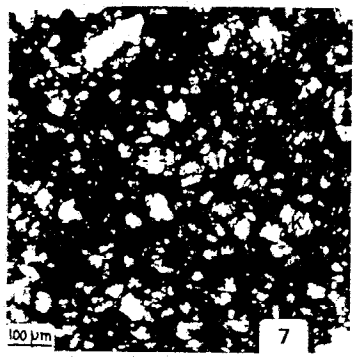

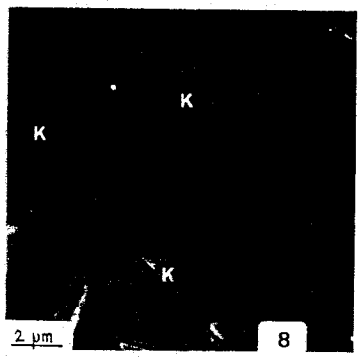

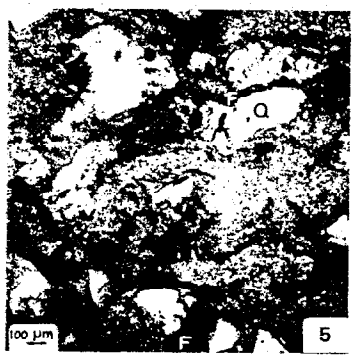

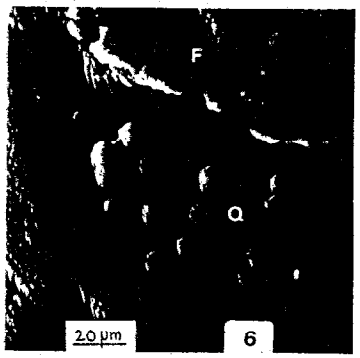

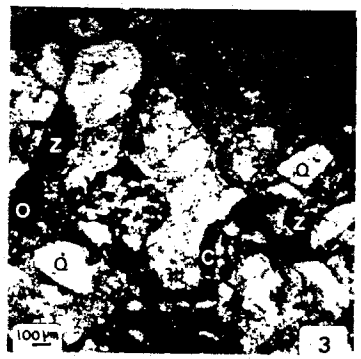

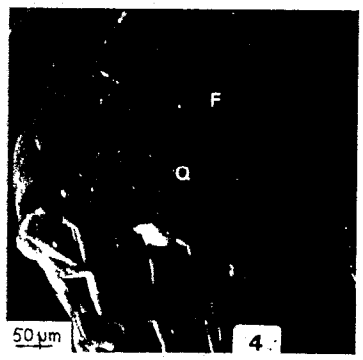

PLATE II - EVOLUTION OF THE MATRIX OF SEDIMENTARY ORIGIN IN THE NODULAR LEVEL (from 9 to 2.5 meters): FERRUGINOUS NODULATION.

Photos 9 and 10. Thin section micrograph (plain light): neoferrans (F) around quartz grains (Q) and voids (V).

Photo 11. Thin section micrograph (plain light): iron concentrations (F) around the grains and the voids and in the form of irregularly distributed speks.

Photo 12. Thin section micrograph (crossed nicols): strong corrosion of the quartz (Q) with ferric incrustations (F). Crystic plasmic fabric (C) in the intergranular material (gibbsite) and dissolution vughs (V).

Photo 13. Thin section micrograph (crossed nicols): general view of crystic fabric (C) in intergranular material, neoferrans (F) around quartz grains (Q) bordered by voids (V) as a result of dissolution.

Photo 14. SEM: gibbsite crystallaria (G), ferriargillans (F).

PLATE II

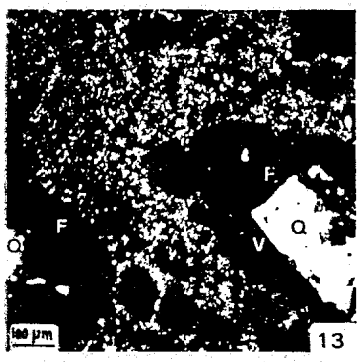

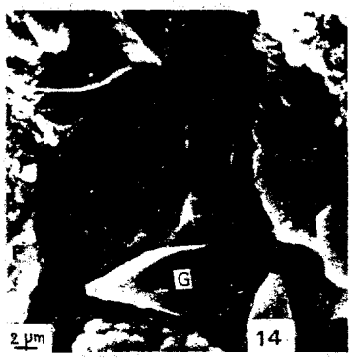

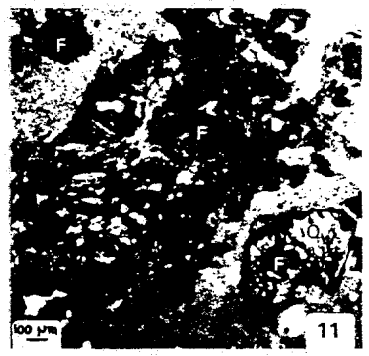

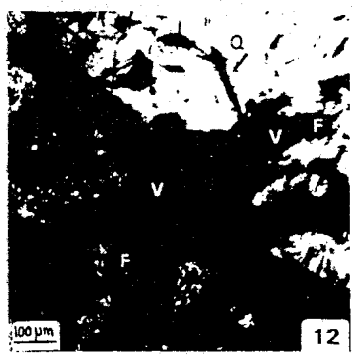

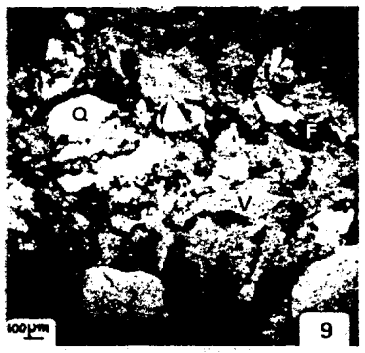

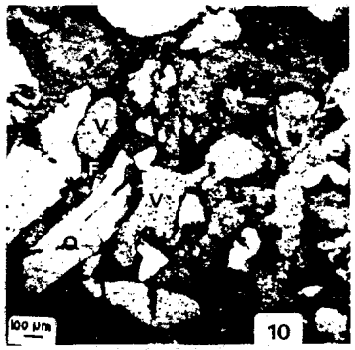

PLATE III - EVOLUTION OF SECONDARY ACCUMULATIONS OF KAOLINITE IN THE NODULAR LEVEL (from 9 to 2.5 meters depth): GIBBSITIC NODULATION.

Photo 15. Thin section micrograph (crossed nicols): secondary accumulation of neoformed kaolinite (K).

Photo 16. SEM: secondary accumulation of automorphic neoformed kaolinite (K).

Photo 17. Thin section micrograph (crossed nicols): gibbsite (G) crystallization in secondary accumulations of kaolinite.

Photo 18. SEM: small kaolinite aggregates (K), covered by very fine goethite crystals (g), and gibbsite crystals (G).

Photo 19. Thin section micrograph (crossed nicols): microcrystalline gibbsite nodules and gibbsite crystallaria.

Photo 20. SEM: crystalliplasma composed of gibbsite (G) and kaolinite (K).

PLATE III

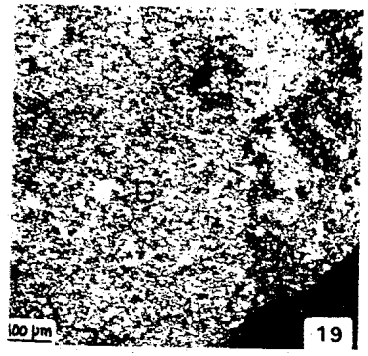

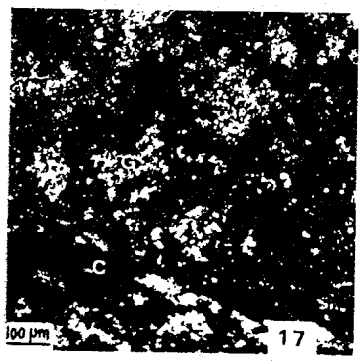

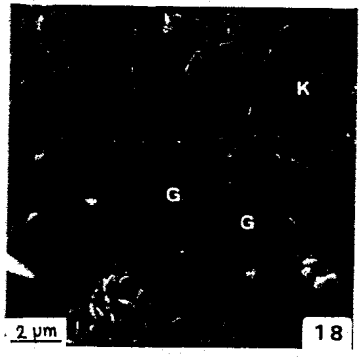

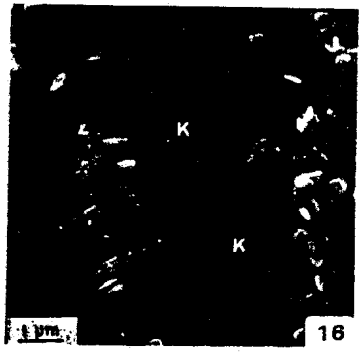

PLATE VI - FORMATION OF PERINODULAR FISSURES AND PROGRESSIVE SUBSTITUTION OF NODULES BY A PREDOMINANTLY KAOLINITIC S-MATRIX.

Photos 21 and 22. Thin section micrograph (crossed nicols): fissure (V) around ferri-gibbsitic and gibbsitic nodule.

Photo 23. Thin section micrograph (crossed nicols): ferri-gibbsitic nodule (FG), S-matrix predominantly kaolinitic, with disseminated micro-crystals of gibbsite.

Photo 24. SEM: kaolinite plasma with some gibbsite crystals.

Photos 25 and 26. Thin section micrograph (plain light and crossed nicols): light coloured gibbsitic volumes (G) in predominantly kaolinitic S-matrix (K), radial fissures resulting from kaolinite shrinkage (V).

PLATE IV

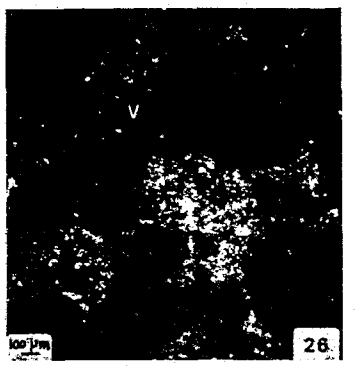

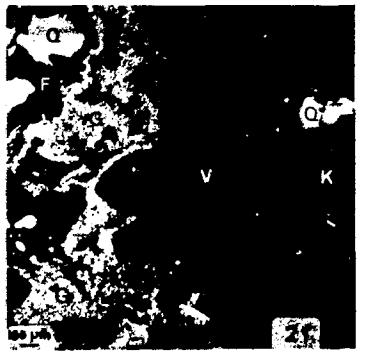

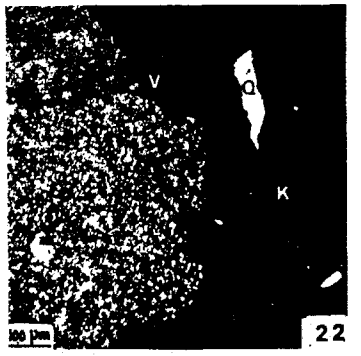

PLATE V - DISTURBANCE OF SOIL MATERIAL (PEDOTURBATION) (from 5.5 to 0 meters).

Photo 27. Thin section micrograph (plain light): microaggregates (MA) of predominantly kaolinitic S-matrix, quartz (Q), interpedal lobated voids (V), ferruginous (F) and gibbsitic (G), micronodules.

Photo 28. SEM: plasmic structure of bioturbed plasma, fine particle of kaolinite (K) and of gibbsite (G).

Photo 29. Thin section micrograph (plain light): bioturbed S-matrix inside of which small grains of quartz (Q) and ferric and gibbsitic (G) are disseminated.

Photo 30. Thin section micrograph (plain light): pedotubules (P) outlining the contours of a gibbsitic nodule (G).

Photo 31. Thin section micrograph (plain light): kaolinitic S-matrix with disseminated quartz (Q) and zircon (Z) grains.

Photo 32. Thin section micrograph (crossed nicols): very corroded quartz grain (Q); the fragments derived from the same parent grain present the same crystallographic orientation.

PLATE V

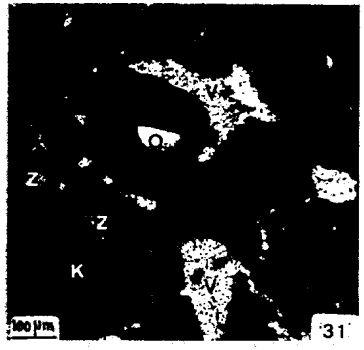

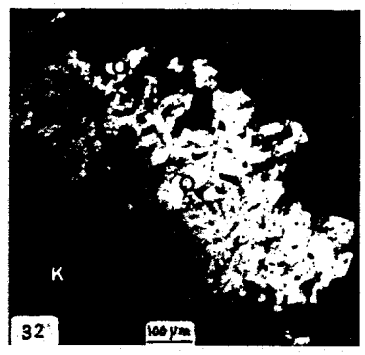

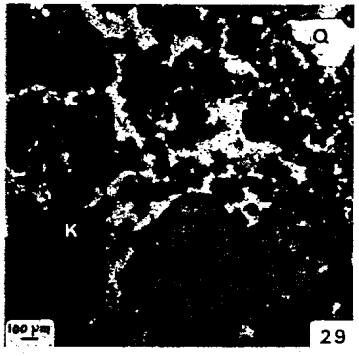

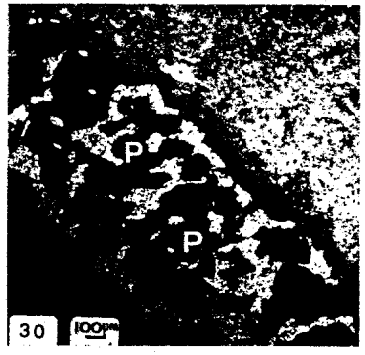

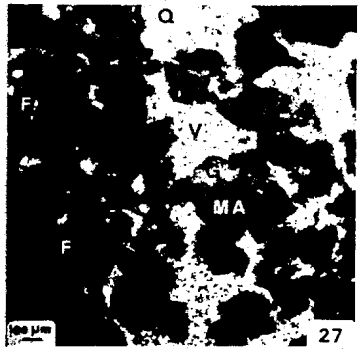

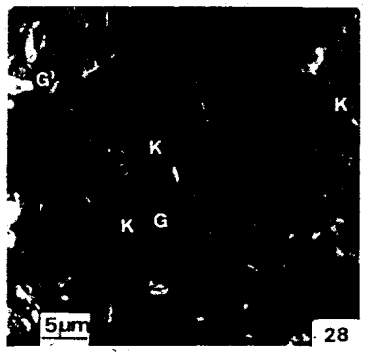

CONCLUSIONS

The ferruginous and gibbsite nodules are first formed, and then destroyed at a later stage, in situ, with the deepening of both the weathering and the pedologic profiles and the lowering of the topographic surfaces developed upon the Barreiras group sediments. Originating from the matrix of sedimentary origin and from secondary accumulations of kaolinite at the base of the profile, these nodules give rise, in turn, to the clayey S-matrix of the B2 horizon.

Geochemically, this evolution consists of the desilicification of quartz and phyllosilicates, which leads to the formation of segregated aluminum and iron oxi-hydroxides. These oxi-hydroxides are destroyed by weathering at the top of the nodular level and contribute, lower in the profiles and topographically, to the formation of a plasma made up of kaolinite and of iron hydroxide.

ACKNOWLEDGEMENTS

The authors are indebted to Professors Fairchild and Nahon for their helpful and critical suggestions. We thank also Dr. Pedro and J. Berrier for their collaboration in SEM observation and interpretation.

REFERENCES

. Bigarella, J.J., 1975. The Barreiras group in Northeastern Brazil. In Simpósio Internacional sobre o Quaternário. Anais Acad. Bras. Ciênc., v. 47 (supl.): 365-393.

. Brewer, R., 1964. Fabric and mineral analysis of soils. John Wiley and Sons, New York, 470 p.

. EMBRAPA, 1981. Mapa de Solos do Brasil. Escala 1:500.000.

. Hole, F.D., 1961. A classification of pedoturbations and some other processes and factors of soil formation in relation to isotropism and anisotropism. Soil Sci., 19: 375-377.

. Join, P., 1980. Caractérisation de nodules gibbsitiques du basin de l'Amazone. Mémoire du DEA de Pédologie, Paris VII, 23 p.

. Muller, D., Bocquier, G., Nahon, D., Paquet, H., 1980/1981. Analyse des differenciations mineralogiques et structurales d'un sol ferralitique à horizons nodulaires du Congo. Cah. ORSTOM, sér. Pédol., vol. XVIII, nº 2: 87-109.

. Sioli, H., 1968. Hydrochemistry and geology in the Brazilian Amazon region. Amazoniana, 1, 3: 267-277.

. Sombroek, W.G., 1966. Amazon soils: a reconnaissance of soils of the Brazilian Amazon region. Center of Agricultural Publication and Documentation, Wageningen-Holland, 292 p.

. Truckenbrodt, W., Kotschoubey, B., 1981. Argila de Belterra, cobertura terciária das Bauxitas Amazônicas. Rev. Bras. Geociências, 11(3): 203-208.